IMPACT: International Journal of Research in Engineering & Technology (IMPACT: IJRET)
ISSN(E): 2321-8843; ISSN(P): 2347-4599
Vol. 2, Issue 6, Jun 2014, 85-98

VARIATION IN BEARING CAPACITY OF FOOTING ON SLOPPING ANISOTROPIC ROCK MASS

D. K. SHUKLA[1], MAHENDRA SINGH[2] & K. K. JAIN[3]

[1,3]Department of Civil Engineering, Jaypee University of Engineering and Technology, Guna, Madhya Pradesh, India

[2]Department of Civil Engineering, Indian Institute of Technology, Roorkee, Uttarakhand, India

ABSTRACT

The rock mass bearing capacity and its deformational behavior is governed by the interaction of intact blocks with the discontinuities in rock mass. Under very low confining pressure or unconfined stress condition, they dictate a major influence on strength and deformational behavior of the jointed rock mass. In this study, strength and deformational behavior of slopping anisotropic rock mass have been assessed experimentally as well as analytically. The jointed rock mass assembled using sand stone element of 25 mm × 25 mm × 75 mm along different joint angles of 15˚, 30˚, 45˚, 60˚, 75˚ and 90˚ and slope angles of 30˚, 45˚, 60˚, 75˚, and 90˚ with the horizontal in plane strain condition and 15 cm × 15 cm footing placed exactly at the edge of the slope as well as at 15 cm from edge. Joint angle, distance of footing from edge and modes of failure are important parameters, which govern the load intensity at slope apart from rock mass properties. Load carrying capacity of rock mass can be assessed analytically, if the mode of failure can be predicted. Unconfined rock mass with continuous joint parallel to side slope predicts buckling failure which is also observed experimentally. Experimental data has been analyzed by Euler's buckling theory as suggested by Cavers (1981).

KEYWORDS: Bearing Capacity, Slopping Anisotropic Rock Mass, Plain Strain, Edge Distance, Failure Modes, Rock Mass Buckling

INTRODUCTION

The discontinuities in general and joints in particular are the inevitable part of rock mass encountered in almost all civil engineering and mining engineering projects. A foundation on rock, therefore, should be designed with as much care as a foundation on soil. Most of the methods available for finding the ultimate bearing capacity of jointed rock mass considering the mass as an isotropic medium [8, 9]. The applicability's of these methods will remain doubtful for anisotropic rock mass. Methodologies suggested for jointed rock mass are those proposed by the Hoek-Brown failure criterion for rocks and rock masses are most widely used non-linear criterion world over. Anisotropic rock mass bearing capacity given by Ramamurthy and Arora predicted on the basis of joint factor, Singh and Rao, predicted on the basis of Bell's approach using joint factor [11]. All the methods mentioned above give reasonably good results for confined rock mass. However, these theories are not suitably applicable for unconfined rock mass.

The bearing capacity of rock mass at slope usually assessed by empirical equations [5], design charts [2], limiting equilibrium method or plasticity equations [9.12]. Jointed rock mass bearing capacity in confined and unconfined condition could be assessed accurately only after determination of uniaxial compressive strength (σ_{cj}), modulus of elasticity of rock mass, angle of joint plane with loading direction, type of failure and other rock mass properties

Adhikary et al. (2001) devised on large deformation model of rock masses with elastic layers of equal mechanical properties and equal thickness on the basis of Cosserat continuum theory in to finite element code. A design chart given by them suitable for assessing the stability of foliated rock slopes in dry state. Pore water as well as cross jointing in not considered by Adhikary et al. (2001) Stability analysis and stabilisation of toppling failure by Mehdi Amini et. al. (2009) presented an analytical method for the determination of the magnitude and point of application of inter column forces in rock mass with a potential of flexural buckling. A simple approach to analyse buckling of a rock slope was presented by Cavers (1981) considered flexural buckling of plane slab, three hinges buckling of plane and curve slopes.

In the present study, bearing capacity at slope edge and at 150 cm from edge have been assessed by experimental verification with the objective to find out the resistance to failure is given by rock mass and the modes of failure. Experiments were conducted on anisotropic rock mass in plane strain condition. Experimental results have been compared with analytical results obtained on the basis of mode of failure.

Though the natural configuration of jointed rock mass in the field is not possible to generate in the laboratory, sand stone elements of size 25 mm × 25 mm × 75 mm is used to assemble jointed rock mass. So far only artificial material has been used by researchers. Experiments were conducted in a specially designed and fabricated bearing capacity test apparatus of 200 ton capacity. The rock mass model dimensions 750 mm × 750 mm ×150 mm are considered large enough to nullify the scale effect.

ROCK MASS BEARING CAPACITY THEORIES

Hoek-Brown Failure Criteria for Rock Masses

The Hoek-Brown failure criterion for rocks and rock masses is the most widely used non-linear criterion world over. It was originally suggested in Hoek E. 1980 [5] and subsequently updated in Hoek E, Brown E T(1988)[7], Hoek E, and Brown E T. (1997)[8], Hoek, E.(2000)[9], Hoek E, Carranza-Torres C, and Corkum B. (2002) [10], Hoek E, Marinos P, and Marinos V (2005) [11], respectively by incorporating the experience gained by the authors and other researchers in using the criterion.

Cavers D S (1881)

Cavers (1981) [6] predicted buckling modes of failure are a possibility whenever a continuous joints approximately parallel to the slope, separates a thin slab. The maximum load that can be carried per unit width, before buckling takes place, is as given by Cavers (1981) [6] for flexural buckling of plane slabs by classical buckling theory.

$$\frac{P_{cr}}{B} = \frac{K\pi^2 E_j I}{BL_b^2} \quad (1)$$

Application of Eulers formula for a slope requires additional assumptions for buckling length. According to Cavers (1981), the driving force given as

$$P_D = (W_D \sin\alpha - W_D \cos\alpha \tan\phi_j - l_D C)b \quad (2)$$

These results should form upper and lower bound on l_b/l for the conditions and material used. For rock $l_b/l = 0.5$ and substituting the slab dimensions and unit weight (γ) in equation (2) becomes as

$$\frac{P_D}{b} = 0.75ld\left(\gamma \sin\alpha - \gamma \cos\alpha \tan\phi_j - C/d\right) \quad (3)$$

Ramamurthy and Arora (1994)

Arora (1987) [3] and Ramamurthy and Arora (1994) [4] provided solution for determination of unconfined compressive strength through concept of joint factor. They give maximum importance to joint frequency, joint inclination and joint strength for predicting behavior of jointed rocks. By clubbing these three parameters, a factor called Joint Factor (J_f) was been defined as.

$$J_f = \frac{J_n}{nr} \tag{4}$$

Where, J_n = Number of joints per meter in the direction of major principal stress,

n = Inclination factor which depends on orientation of joint with respect to loading direction,

r = Joint strength parameter = $\sigma_{cj} / \sigma_{ci} = tan\, \emptyset_j$

$\emptyset_j$ = Discontinuity friction angle

The value of J_f thus obtained is an indicative of how much weakness has been brought to intact rock by presence of joints. The value of 'n' is given in the table 1. Values of 'r' have to be determined by conducting direct shear test.

Table 1: Values of Inclination Parameter, n for Different Joint Orientation, β^o from Ramamurthy and Arora (1994)

Orientation of Joint (βo)	0	10	20	30	40	50	60	70	80	90
Inclination parameter (n)	0.814	0.460	0.105	0.046	0.071	0.306	0.465	0.634	0.814	1.000

The average value of strength of the jointed rock mass is the unconfined compressive strength of the jointed rock mass that is given as

$$q_u = \sigma_{cj} = \sigma_{ci} \exp\left(-0.008 J_f\right) \tag{5}$$

Singh and Rao (2005)

Singh and Rao (2005) [18] suggested a procedure to estimate the ultimate bearing capacity of shallow foundation in anisotropic rock masses. The approach considers the strength properties of the mass as a whole, which depends both on joint properties and intact rock properties. Bell"s approach has been used for computing bearing capacity, in which the ultimate bearing capacity is determined as a major principal stress at failure under confining pressure acting on the mass beneath a smooth foundation. To define the strength of the rock mass, a simple parabolic equation derived based on critical state of rock has been used. The uniaxial compressive strength of jointed rock mass, which is an input parameter to the strength criterion, is determined using the joint factor concept. As per this approach, the active and passive zones develop in the rock mass under a smooth strip footing. It is assumed that these zones are divided by a vertical line passing through the edge of the footing. The length of the strip footing is assumed to be infinite and the ground surface is horizontal. The rock mass under the footing, as well as the adjacent mass, is assumed to be in a triaxial stress state. The major principal stress for the active zone just beneath the footing, acts in vertical direction. For the passive zone, the major principal stress acts in the horizontal direction and the effective surcharge acts as the minor principal stress. At the time of failure, equilibrium of two adjacent elements of rock prisms is considered, one just beneath the edge of the footing (Element II) and the other just outside (element I) figure 1.

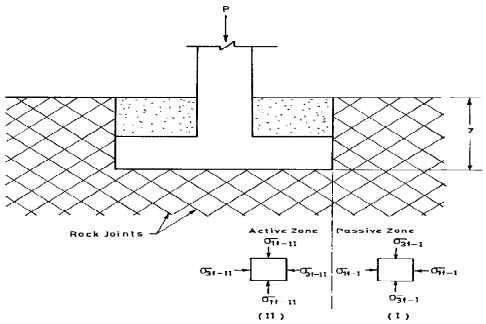

Figure 1: Bell's Approach for Bearing Capacity

For element-I (adjacent element), at the time of failure:

$$\sigma_{3-1} = \gamma z \; and \; \sigma_{1-1} = f(\sigma_{3-1}) \tag{6}$$

where γ = unit weight of the rock mass,

z = depth of the foundation,

$\sigma_{3\text{-}I}$ = confining stress acting on element I at the time of failure and

$\sigma_{1\text{-}I}$ = major principal stress at element I at the time of failure.

For element II (element below the footing), at the time of failure:

$\sigma_{3\text{-}II}$ = confining stress = $\sigma_{1\text{-}I}$

σ 1-II = major principal stress for element II at the time of failure,

The ultimate bearing capacity is given as:

$$q_{ult} = \sigma_{1-II} \tag{7}$$

The uniaxial compressive strength σ_{cj} depends on the Joint Factor J_f and the mode of failure (Singh et al., 2002). Its value is estimated as:

$$\sigma_{cj} = \sigma_{ci} \exp(aJ_f) \tag{8}$$

where a is an empirical coefficient depending on failure mode as presented in Table 2

Table 2: Coefficient 'a' for Estimating σ_{cj}

Failure Mode	Coefficient "a"
Splitting/ Shearing	- 0.0123
Sliding	-0.0180
Rotation	-0.0250

The strength may be computed for these extreme values, and for intermediate values of σ, linear interpolation can be made.

Modulus of Jointed Rocks

Ramamurthy and Arora 1993 [4], the ratio of moduli of jointed rock and that of the intact rock in uniaxial compression was linked to the joint factor.

$$E_r = \frac{E_j}{E_i} = \exp\left(-1.15 \times 10^{-2} J_f\right) \quad (9)$$

Experimental Details

Carefully planned specific experimental program was executed to achieve the objective of the study. A 200 ton bearing capacity test apparatus shown in the figure 2 for testing the rock mass in plane strain conditions is designed and fabricated. The vertical load observed by proving ring placed over jack and vertical displacement was recorded at all four corner of footing during testing of the specimen up to failure. Perspex transparent sheet is fixed on the front side to observe the failure pattern; Steel plates were fixed on the other two sides. Approximately 2000 to 2400 number of blocks were required to form one blocky mass.

Figure 2: Bearing Capacity Test Apparatus (J0090-SL45-ED00)

Element joint angle was varied from 0°, 15° 30° 45° 60° 75° to 90° whereas side slope inclination also varied from 90º, 75°, 60°, 45° to 30° with horizontal as shown in figure 3. For side slope 15° experiments were not conducted because it approached almost flat. 150 mm × 150 mm footing was placed exactly on the edge of the rock mass.

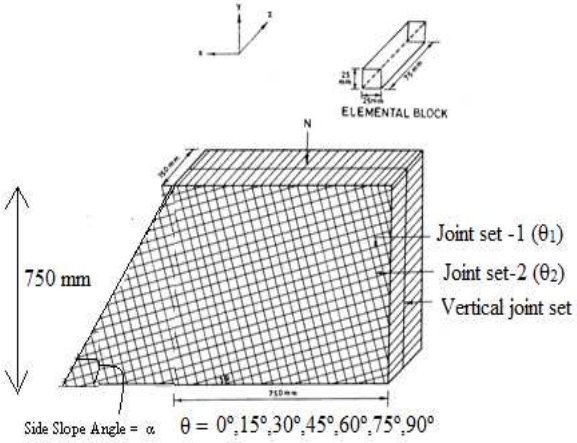

Figure 3: Rock Mass Arrangements with Variation in Joint Set Angle and Side Slope

An experiment is designated as J4545-SL45-ED15 which indicates that joint set-1angle (θ_1) is 45° with the horizontal and joint set-2 angle (θ_2) 45°, side slope angle (α) 45° and distance footing from edge 15 cm as shown in figure 3. The size of the rock mass specimen was kept as 750 mm x 750 mm x 150 mm while the size of elemental blocks used was 25 mm x 25 mm x 75 mm as shown in figure 4.

Figure 4: For Joint Angle 45º-45º, Side Slope 45º and Edge Distance 15 cm (J4545-SL45-ED15)

Model Material

Sand stone is used to make the elements as model material. Physical and the engineering properties of the model material are presented in Table 3. These properties are obtained as per Indian standard procedure using code as IS 9221-1979, IS-10082-1982, IS-13030-1991. Average uniaxial compressive strength of the intact material has been found to be 48.5 MPa. Failure strain of the intact material has been found to be 0.81 % and the tangent modulus obtained at 50% of failure stress was observed to be 8773 MPa. The modulus ratio, Et50/σci, of the material is found to be 181.

The value of basic friction angle of joint (φj) was found as 29º by direct shear test. Shear strength parameters for intact material (ci and φi) were obtained by conducting triaxial tests under varying confining pressures i.e. at σ_3 = 2.45 MPa, 4.9 MPa 7.35 MPa and 14.7 MPa respectively.

Table 3: Physical and Engineering Properties of the Model Material

S N	Property	Value
1	Dry unit weight, γd (kN/m^3)	24.91
2	Specific gravity, G	2.52
3	Uniaxial Compressive Strength, σ_{ci} (MPa)	48.5
4	Failure strain, ε_f (%)	0.81
5	Tangent modulus, E_{t50} (MPa)	8773
6	Tangent modulus, E (MPa)	5820
7	Brazilian strength, σ_t (kN)	15.8
8	Friction angle of joint, φ_j (degree)	30
9	Friction angle of intact model material, φ_i (degree)	39
10	Cohesion of intact model material, c_i (MPa)	19

EXPERIMENTAL RESULTS AND OBSERVATION

Experimental Results

Experiments were conducted by placing the footing placed at edge and at 15 cm from edge. Failure load and deformation at all four corners of the footing are measured. The mode of failure was observed either buckling or a combination of buckling and sliding failure in most of the tests. For joint angle 00º- 90º and joint 15-75 buckling failure observed, whereas for joint 30º-60º, 45º-45º and 60º-30º initially sliding and finally buckling take place. Load intensities were 20-100 times less than its unconfined compressive strength. Experimental results shows footing settlement and load intensity increases with decrease in side slope angle with horizontal Experimental results have shown in table 4 and 5 below.

Table 4: Experimental Results at Edge

S N	Test	Load Intensity (MPa)	Average Settlement (mm)	**Buckling Length (mm)
1	J0090-SL90-ED00	1.39	1.75	675
2	J0090-SL75-ED00	2.92	2.95	625
3	J0090-SL60-ED00	2.81	2.86	625
4	J0090-SL45-ED00	2.82	3.27	625
5	J0090-SL30-ED00	2.92	4.58	675
6	J1575-SL90-ED00	0	0	0
7	J1575-SL75-ED00	1.17	4.63	750
8	J1575-SL60-ED00	1.94	4.15	675
9	J1575-SL45-ED00	2.59	11.20	650
10	J1575-SL30-ED00	2.92	7.88	625
11	J3060-SL90-ED00	0	0	0
12	J3060-SL75-ED00	0	0	0
13	J3060-SL60-ED00	0.52	3.69	875
14	J3060-SL45-ED00	0.52	8.63	850
15	J3060-SL30-ED00	1.06	4.25	850
16	J4545-SL90-ED00	0	0	0
17	J4545-SL75-ED00	0	0	0
18	J4545-SL60-ED00	0	0	0
19	J4545-SL45-ED00	0.52	9.88	1075**
20	J4545-SL30-ED00	0.63	10.66	1075**
21	J6030-SL90-ED00	0	0	0
22	J6030-SL75-ED00	0	0	0
23	J6030-SL60-ED00	0	0	0
24	J6030-SL45-ED00	0	0	0
25	J6030-SL30-ED00	0.11	5.06	1500**

Table 5: Experimental Results at 15 cm from Edge

S N	Test	Load Intensity (MPa)	Average Settlement (mm)	**Buckling Length (mm)
1	J0090-SL90-ED15	5.54	5.33	550
2	J0090-SL75-ED15	5.76	6.01	575
3	J0090-SL60-ED15	7.72	5.83	475
4	J0090-SL45-ED15	7.29	6.21	450
5	J0090-SL30-ED15	7.51	8.15	475
6	J1575-SL90-ED15	0	0	0
7	J1575-SL75ED15	3.14	6.45	575
8	J1575-SL60-ED15	3.03	7.13	675
9	J1575-SL45-ED15	3.36	7.72	650
10	J1575-SL30-ED15	4.45	6.16	600
11	J3060-SL90-ED15	0	0	0
12	J3060-SL75-ED15	0	0	0
13	J3060-SL60-ED15	0.95	4.80	875
14	J3060-SL45-ED15	1.39	11.46	875
15	J3060-SL30-ED15	1.17	8.13	875
16	J4545-SL90-ED15	0	0	0
17	J4545-SL75-ED15	0	0	0
18	J4545-SL60-ED15	0	0	0
19	J4545-SL45-ED15	0.41	9.02	1075
20	J4545-SL30-ED15	0.63	10.66	1075
21	J6030-SL90-ED15	0	0	0
22	J6030-SL90-ED15	0	0	0
23	J6030-SL90-ED15	0	0	0

Table 5: Contd.,

24	J6030-SL90-ED15	0	0	0
25	J6030-SL90-ED15	0.19	1.22	1500

Note: * Settlement recorded at all four corner of footing. Average of all four dial gauge readings is given
** Buckling Length L_b is measured on the basis of rock specimens shifted from its original position at failure
*** If a combination of sliding and buckling failure occurred than entire slope length taken as buckling length

Observations

Joint Angle 00º-90º (J0090)

A zone of compression has been observed with vertical joints opened up just below footing. Vertical joints opening commenced from centre of footing towards unconfined side. Finally buckling failure takes place. Average footing settlement observed minimum 1.71 mm for the side slope 90º and maximum 4.58 mm for the side slope 30º respectively. Load intensities were as low as 1.39 MPa for the side slope 90 and maximum 2.92 MPa for the side slope 30º at edge similarly when footing placed at 15 cm from edge the average footing settlement observed minimum 5.33 mm for the side slope 90º and maximum 8.15 mm for the side slope 30º respectively. Load intensities were as low as 5.54 MPa for the side slope 90 and maximum 7.72 MPa for the side slope 60º which is little greater than the load intensity at side slope 30º.

Joint Angle 15º-75º (J1575)

A little zone of compression has been observed with vertical joints opened up just below footing in the direction of vertical plane. Side slope 90º with joint angle 15º-75º (J1575-SL90-ED00) gave zero load intensity because elements sliced by its own weight. Vertical joints opening commenced from centre of footing towards unconfined side. Finally buckling failure takes. At edge average footing settlement observed as minimum 4.15 mm for the side slope 60º and maximum 11.2 mm for the side slope 45º. Load intensities were as low as 0 MPa for the side slope 90 and maximum 2.92 MPa for the side slope 30º and when footing placed at 15 cm from edge average footing settlement observed as minimum 6.16 mm for the side slope 30º and maximum 7.72 mm for the side slope 45º. Load intensities were as low as 3.03 MPa for the side slope 60 and maximum 4.45 MPa for the side slope 30º.

Joint Angle 30º-60º (J3060)

No zone compression observed below the base footing. In the beginning as the load applied elements below the base of footing sliced in the direction of joint angle. The magnitude of load intensities were governs by toe resistance (Toe support is provided). Finally vertical joints opened up and buckling takes. Load intensities were negligible in sliding (toe support not provided). At edge, average footing settlement observed minimum 3.69 mm for the side slope 60º and maximum 8.63mm for the side slope 45º. Load intensities were as low as 0 MPa for the side slope 90º and 75º and maximum 1.06 MPa for the side slope 30º footing placed at edge. At 15 cm distance, average footing settlement observed as minimum 4.8 mm for the side slope 60º and maximum 11.46 mm for the side slope 45º. Load intensities were as low as 0 MPa for the side slope 90º and 75º and maximum 1.39 MPa for the side slope 45º.

Joint Angle 45º-45º (J4545)

No zone compression observed below the base footing. In the beginning as the load applied elements below the base of footing sliced in the direction of joint angle. The magnitude of load intensities were governs by toe resistance (Toe support is provided). Finally vertical joints opened up and buckling takes. Load intensities were negligible in sliding

(toe support not provided). At edge, average footing settlement observed as minimum 9.88 mm for the side slope 45º and maximum 10.66 mm for the side slope 30º. Load intensities were as low as 0 MPa for the side slope 90º, 75º, 60º and maximum 0.63 MPa for the side slope 30º. At 15 cm from edge, average footing settlement observed as minimum 9.02 mm for the side slope 45º and maximum 10.66 mm for the side slope 30º. Load intensities were as low as 0 MPa for the side slope 90º, 75º, 60º and maximum 0.63 MPa for the side slope 30º.

Joint Angle 60º-30º (J6030)

No zone compression observed below the base footing. In the beginning as the load applied elements below the base of footing sliced in the direction of joint angle. At edge, momentarily buckling failure takes place towards unconfined side. Load intensities were as low as 0 MPa for the side slope 90º, 75º, 60º, 45º and maximum 0.19 MPa for the side slope 30º. At 15 cm from edge, load intensities were as low as 0 MPa for the side slope 90º, 75º, 60º, 45º and maximum 0.19 MPa for the side slope 30º.

Analysis of Results

As per classical buckling theory (Euler's method) it is assumed that column is straight, weightless, elastic and obeys Hook's law. As observed from experiments either buckling or a combination of sliding and finally buckling take place. For the analysis of results buckling length has been observed from pictures / video taken at the time experiments at failure. In the case of a combination of sliding and buckling failure takes place then entire slope length is considered as buckling length because if rock mass is free to slide then sliding take place or if rock mass restricted at toe then buckling will take place from toe. Analytical results have been given in table 6 and table 7.

Table 6: Comparison of Buckling Load Intensity, Calculated and Experimental Results at Edge

S N	Test	P_{cr}	Calculated Load Intensity (MPa)	Experimental Load Intensity (MPa)	Corrected Load** Intensity (MPa)
1	J0090-SL90-ED00	6969.37	0.93	0.98	1.86
2	J0090-SL75-ED00	8129.07	2.17	2.84	2.17
3	J0090-SL60-ED00	8129.07	2.17	1.97	2.17
4	J0090-SL45-ED00	8129.07	2.17	2.16	2.17
5	J0090-SL30-ED00	6969.37	1.86	2.37	1.86
6	J1575-SL90-ED00	0.00	0.00	0.00	0.00
7	J1575-SL75-ED00	4998.09	1.33	1.09	1.29
8	J1575-SL60-ED00	6170.48	1.65	1.86	1.59
9	J1575-SL45-ED00	6654.26	1.77	2.73	1.71
10	J1575-SL30-ED00	7197.25	1.92	2.83	1.85
11	J3060-SL90-ED00	0.00	0.00	0.00	0.00
12	J3060-SL75-ED00	0.00	0.00	0.00	0.00
13	J3060-SL60-ED00	1988.60	0.53	0.437	0.46
14	J3060-SL45-ED00	2107.29	0.56	0.437	0.49
15	J3060-SL30-ED00	2107.29	0.56	0.98	0.49
16	J4545-SL90-ED00	0.00	0.00	0.00	0.00
17	J4545-SL75-ED00	0.00	0.00	0.00	0.00
18	J4545-SL60-ED00	0.00	0.00	0.00	0.00
19	J4545-SL45-ED00	437.42	0.12	0.54	0.08
20	J4545-SL30-ED00	437.42	0.12	0.33	0.08
21	J6030-SL90-ED00	0.00	0.00	0.00	0.00
22	J6030-SL75-ED00	0.00	0.00	0.00	0.00
23	J6030-SL60-ED00	0.00	0.00	0.00	0.00

Table 6: Contd.,

24	J6030-SL45-ED00	0.00	0.00	0.00	0.00
25	J6030-SL30-ED00	0.00	0.00	0.19	0.00

* Buckling Length L_b is measured on the basis of rock specimens shifted from its original position at failure
** Calculated load intensity is resolved in vertical direction according to joint angle
*** In case of sliding and buckling occurred simultaneously than entire slope length taken as buckling length

Experiments analyzed for footing at edge as well as at distance B (15 cm) from edge below.

Table 7: Comparison of Buckling Load Intensity, Calculated and Experimental Results at 15 cm from Edge

S N	Test	P_{cr}	Calculated Load Intensity (MPa)	Experimental (MPa)	Corrected** Load Intensity (MPa)
1	J0090-SL90-ED15	10499.65	5.60	5.54	5.60
2	J0090-SL75-ED15	9606.48	5.12	5.76	5.12
3	J0090-SL60-ED15	14077.09	7.51	7.72	7.51
4	J0090-SL45-ED15	15684.66	8.37	7.29	8.37
5	J0090-SL30-ED15	14077.09	7.51	7.51	7.51
6	J1575-SL90-ED15	0.00	0.00	0.00	0.00
7	J1575-SL75-ED15	8505.3	4.54	3.14	4.38
8	J1575-SL60-ED15	6171.89	3.29	3.03	3.18
9	J1575-SL45-ED15	6655.78	3.55	3.36	3.43
10	J1575-SL30-ED15	7811.3	4.17	4.45	4.02
11	J3060-SL90-ED15	0.00	0.00	0.00	0.00
12	J3060-SL75-ED15	0.00	0.00	0.00	0.00
13	J3060-SL60-ED15	1989.05	1.06	0.95	0.92
14	J3060-SL45-ED15	1989.05	1.06	1.39	0.92
15	J3060-SL30-ED15	1989.05	1.06	1.17	0.92
16	J4545-SL90-ED15	0.00	0.00	0.00	0.00
17	J4545-SL75-ED15	0.00	0.00	0.00	0.00
18	J4545-SL60-ED15	0.00	0.00	0.00	0.00
19	J4545-SL45-ED15	437.52	0.23	0.41	0.16
20	J4545-SL30-ED15	437.52	0.23	0.63	0.16
21	J6030-SL90-ED15	0.00	0.00	0.00	0.00
22	J6030-SL75-ED15	0.00	0.00	0.00	0.00
23	J6030-SL60-ED15	0.00	0.00	0.00	0.00
24	J6030-SL45-ED15	0.00	0.00	0.00	0.00
25	J6030-SL30-ED15	0.00	0.00	0.19	0.00

A calculation for experiment J0090-SL60-ED00 and J4545-SL45-ED00 analyzed for load intensity as per buckling load method.

Analytical Load Intensity for Experiment J0090-SL60-ED00

Modulus of elasticity of rock masses calculated according to Ramamurthy & Rao theory.

J_n = 40 (one element size is 25 mm)

n = 0.814 (Table 1, Ramamurthy and Arora (1994)

Joint strength parameter (r) = $\tan\phi_j$ = 0.577

$J_f = J_n/nr = 85.16$ (10)

Puting the value of J_f in equation- 9 and Modulus of elasticity (E_{t50}) of intact rock from table 3, we have

$$E_r = \frac{E_j}{E_i} = \exp\left(-1.15 \times 10^{-2} J_f\right) \quad (11)$$

E_j = 3294.6 MPa

The buckling load carrying capacity of footing can be calculated using equation-7 we have,

$$\frac{P_{cr}}{B} = \frac{K\pi^2 E_j I}{BL_b^2}$$

Where buckling length L_b = 625 mm taken from figure 5 below

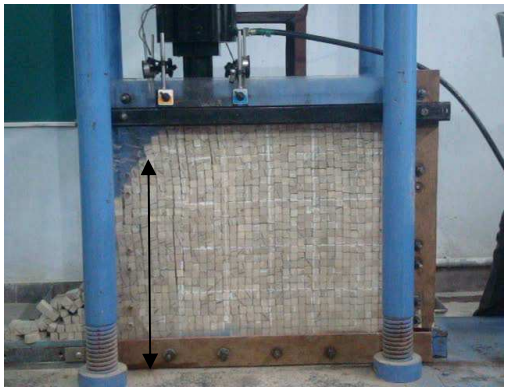

Figure 5: At Failure for the Test J0090SL60ED00

Moment of Inertia = $bd^3/12$, where

B = 15 cm d = 2.5 cm.

I = 19.53 cm^4

Hence we have

P_{cr} = 8129.07× 6 N (Since load is acting at the centre of footing which resulted effective buckling in three rock mass columns out of 12 columns)

Load Intensity = 24387.21/22500

= 2.17 Mpa

Eulers theory P_{cr} = 2.17 > 1.97 MPa (Experimental Value).

Analytical Load Intensity for Experiment J0090-SL90-ED15

Modulus of elasticity of rock masses calculated according to Ramamurthy & Rao theory.

J_f = 40 (one element size is 25 mm)

n = 0.814 (Table 1, Ramamurthy and Arora 199 4) and Joint strength parameter (r) = $\tan\phi_j$ = 0.577

$J_f = J_n/nr$ = 85.16

Puting the value of J_f from equation 10 and Modulus of elasticity (E_{t50}) of intact rock from table 3, we have

$$E_r = \frac{E_j}{E_i} = \exp\left(-1.15 \times 10^{-2} J_f\right) = E_j = 3294.6 \text{ MPa}$$

The buckling load carrying capacity of footing can be calculated using equation-7 we have,

$$\frac{P_{cr}}{B} = \frac{K\pi^2 E_j I}{BL_b^2}$$

Where buckiling length L_b = 550 mm as shown in figure 6 below

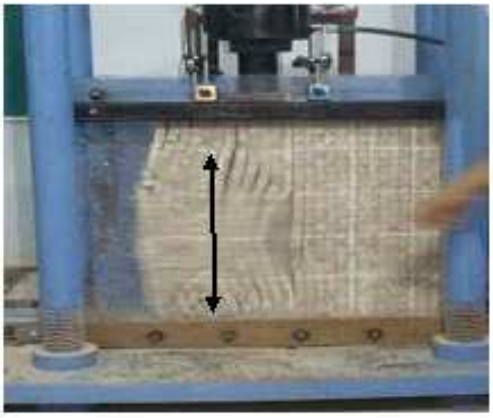

Figure 6: At Failure for the Test J0090-SL90-ED15

Moment of Inertia = $bd^3/12$, where, B = 15 cm d = 2.5 cm and I = 19.53 cm^4, Hence we have

P_{cr} = 10499.65 × 12 N (Since load is acting at the centre of footing which resulted effective buckling in three rock mass columns out of six columns)

Load Intensity = 125995.8/22500 = 5.6 MPa and Corrected for vertical load = 0.12 *cos* (45) = 0.08 MPa

Eulers theory P_{cr} = 5.60 < 5.54 MPa (Experimental Value).

As shown above that Euler's buckling analysis reasonably match the experimental data.

CONCLUSIONS

Bearing capacity of unconfined rock mass with continuous joints at slope edge analyzed by Euler's method of buckling and analytical value nearly match with experimental value. Bearing capacity of jointed rock mass is half of the total buckling load capacity when footing placed at edge of the slope because buckling was observed in outer three columns of unconfined side out of six columns of rock mass below the base footing. Whereas, when footing placed at 15 cm from edge, it is observed all six vertical columns buckled at failure. Average settlement of footing for joint angle (θ) = 0˚, 15˚, 30˚ (Buckling mode of failure) are less than the joint angle (θ) = 45˚, 60˚ (Combination of Sliding and buckling mode of failure) due to mode of failure. Similarly the magnitude of bearing capacity is more for joint angle (θ) = 0˚, 15˚, 30˚ (Buckling mode of failure) as compare to the joint angle (θ) = 45˚, 60˚ (Combination of Sliding and buckling failure). Settlements at failure are more when footing placed at 15 cm distance from edge compared to the footing placed exactly at edge.

ACKNOWLEDGEMENTS

The authors are grateful to Jaypee University of Engineering and Technology, Guna for providing financial assistance and Indian Institute of Technology, Roorkee for valuable support.

REFERENCES

1. Adhikary D P, Muhlhaus H B, Dyskin A V.A numerical study of flexural buckling of foliated rock slopes. *Int. J. Numer. Anal. Meth. Geomech.*, 2001, *25:871-884.*
2. Amini M, Majdi A, Aydan O. Stability analysis and the stabilization of flexural Toppling failure. *Rock mechanics Rock Eng*, 2009, *42-751-78.2*
3. AroraV K, Strength and deformational Behavior of jointed rocks, 1987, Ph. D Thesis, IIT Delhi, India.
4. Arora V K, Ramamurthy T. A Simple approach to predict unconfined compressive strength of jointed rock mass. Proc. of the Asian Regional Symposium on rock slopes. Pub. A A Balkema. Rotterdom, Neth. New Delhi, 1993, pp. 13 BN-90-5410-243.
5. Bindlish A. Bearing capacity of strip footings on jointed rocks. PhD thesis, IIT Roorkee, India, 2007.
6. Cavers D S. Simple methods to analyze buckling of rock slopes. *Rock Mechanics*, 1980, *14, 87-104.*
7. Hoek E. An empirical strength criterion and its use in designing slopes and tunnels in heavily jointed weathered rock. *Proc., 6th Southeast Asian Conf. on Soil Engineering*, Taipei, 111–158. 1980.
8. Hoek, E. Strength of jointed rock masses. *Geotechnique*, 1983, 33-3, 187–223.
9. Hoek E, Brown E T, The Hoek-Brown failure criterion- a 1988 update. Proc. Of 15th Canadian Rock Mechanics Symposium. Rock Engineering for Underground Excavation, J.H. Curran eds. 1082-31-38.
10. Hoek E, and Brown E T. Practical estimates of rock mass strength. *Int. J. Rock Mech. Min. Sci.*, 1997, 34-8, 1165–1186.
11. Hoek, E. *Practical rock engineering*, Ed., http://www.rocscience.com/hoek/ Practical Rock Engineering.asp. 2000
12. Hoek E, Carranza-Torres C, and Corkum B. Hoek-Brown criterion-2002 edition. Proc. NARMS-TAC Conf. Toronto, 2002, 1, 267-273.
13. Hoek E, Marinos P, and Marinos V, Characterization and Engineering Properties of Tectonically Undisturbed but Lithologically varied sedimentary rock masses, *Int. J. Rock Mech. Min. Sci.* 2005, 42(2)277-285.
14. Imani M, Fahimifar A, Sharifzadeh M. Bearing failure modes of rock foundation with consideration of joint spacing. Scientia Iranica A 2012, 19(6), 1411-1421.
15. Ramamurthy T, Arora, V K. Strength prediction for jointed rocks in confined and unconfined states. *Int. J. Rock Mech. Min. Sci. Geomech. Abstr*, 1994, 31-1, 9–22.
16. Singh, M. Engineering behavior of jointed model materials. PhD thesis, IIT, New Delhi, India. 1997.
17. Singh, M, Rao K S. Ramamurthy T. Strength and deformational behavior of a jointed rock mass. *Rock Mech. Rock En.*, 2002, 35-11, 45–64.
18. Singh M, Rao K S, Bearing Capacity of Shallow Foundations in Anisotropic Non-Hoek–Brown Rock Masses. J. Geotech. Geoenviron. Eng., 2005, 131:1014-1023.

APPENDICES

List of Symbols

B = Slope Width

E_i = Young's Modulus intact rock

Ej = Young's Modulus jointed rock mass

E_r = Ratio of moduli

I = Moment of inertia for a mass of slab

J_f = Joint Factor

J_n = Frequency of joints/ m in the direction of loading

K = 1.0 Pin jointed ends

L_b = Length of slope subjected to buckling

n = Joint inclination parameter

P_{cr} = Critical load in flexural buckling

r = Joint strength parameter

σ_{cj} = Uniaxial compressive strength of jointed rock mass

σ_{ci} = Strength of intact rock.

Φ_j = Friction angle along the joint plane.

θ = Joint Angle with the horizontal

α = Side Slope Angle